An Efficient Energetic Variational Principle for Modeling One-Port Lossy Gyrotropic YIG Straight-Edge Resonators

Isabelle Huynen, *Member, IEEE,* Benoît Stockbroeckx, and Guy Verstraeten

***Abstract*—This paper presents a new variational principle for the design of one-port gyrotropic magnetostatic-wave (MSW) resonators. We first prove the stationary character of the magnetic energy in case of a resonator containing lossy gyrotropic media and supporting microwave MSW's. We then show that the variational expression may be successfully used for calculating the input reflection coefficient of a planar multilayered MSW straight-edge resonator (SER). Results obtained using the variational formulation are validated by experiment carried out at X-band. Hence, the resulting model is an efficient tool for designing low-noise wide-band yttrium–iron–garnet (YIG) tuned oscillators.**

***Index Terms*— Anisotropic media, gyrotropism, magnetostatic waves, modeling, variational methods, YIG materials/devices.**

I. Introduction

MAGNETOSTATIC-WAVE (MSW) planar devices including yttrium–iron–garnet (YIG) films operate as frequency-tunable delay lines or resonators in frequency synthesizers, channel filters, and tuned oscillators. The models found in the literature are based for both structures on the characterization of the propagation mechanism of MSW's in a planar YIG film, which is coupled to planar transducers on a substrate. The most important part of the work on MSW devices deals with MSW delay lines, which are designed as transmission devices [1]–[4].

Concerning YIG resonators based on a stationary behavior of MSW's, many efforts have been devoted in the past to the calculation of the resonant frequencies in order to predict spurious interferences between harmonics [5]–[7]: a dispersion relation for the MSW is computed, from which a resonance condition involving the geometry of the resonator is written. Such an approach has been validated by measurements on the resonant frequency of finite-size YIG straight-edge resonators (SER's) [7]. To the best of our knowledge, no formalism has been established for modeling the coupling mechanism between the transducer and the YIG SER, and obtaining, for example, the frequency-dependent one- or two-port scattering parameters of the resonator. Weak coupling occurs when the multilayered resonator is placed close to the transducer, but not above it (edge coupling). We have proposed earlier (for this case) an efficient model based on the computation of a coupling between two transmission lines modeling, respectively, the YIG resonator and its two microstrip accesses [8]. When the resonator is placed on the transducer (one-port top-coupled configuration) the separation into two different transmission lines is not possible because strong coupling does occur. Hence, it seems preferable to use the input admittance formalism; this circuit parameter has to be expressed as a function of the modes of the equivalent cavity formed by the resonator. These modes, however, may be difficult to compute when the cavity is open or has a complicated geometry. Another difficulty arises from the fact that existing formulations for the input admittance are usually limited to Hermitian media: in particular, perturbational and variational formulations available for this parameter are not applicable to YIG SER's because of the presence of non-Hermitian and inhomogeneous media [9]–[11].

In this paper, we develop an energetic formulation for the computation of the reflection coefficient of a planar one-port SER YIG resonator "top-coupled" onto a microstrip line. We first show that the energy associated with MSW is variational even in the case of lossy gyrotropic, thus non-Hermitian magnetic materials. Our formulation is more general than quasi-static variational principles, which require that the media are at most Hermitian [12]. We transpose the electrostatic variational energetic formulation valid for homogeneous isotropic media into a magnetic energetic formulation for inhomogeneous microwave planar structures including gyrotropic lossy layers, and we extend to this dynamic lossy gyrotropic case the proof of stationary behavior valid for the electrostatic homogeneous case. The resulting formulation is well suited for the modeling of forward magnetostatic volume waves resonators developed for YIG-tuned oscillator (YTO) designs, as illustrated in a following section.

Manuscript received February 18, 1997; revised April 7, 1998. This work was supported in part by Alcatel-Bell, Antwerp, Belgium, the European Space Agency, Estec, The Netherlands, the National Fund for Scientific Research, Belgium, and by the PAI Program, Federal Office for Scientific, Technical and Cultural Matters, Belgium.

I. Huynen and B. Stockbroeckx are with Microwaves, Université Catholique de Louvain (UCL), B-1348 Louvain-la-Neuve, Belgium.

G. Verstraeten is with the Space Systems Department, Alcatel-Bell, B-2660 Hoboken, Belgium.

Publisher Item Identifier S 0018-9480(98)04959-X.

II. Development of the Energetic Variational Formulation

A. MSW Assumption

We consider the whole space, containing several bodies having different permittivities and permeabilities. Maxwell's equations in the ith medium are rewritten using the MSW

hypothesis as

$$\nabla \times \overline{E}_i = -j\omega \overline{B}_i \tag{1a}$$

$$\nabla \times \overline{H}_i = \overline{J}_i \tag{1b}$$

$$\nabla \cdot \overline{B}_i = 0 \tag{1c}$$

with the constitutive relationship

$$\overline{B}_i = \mu_o \overline{\overline{\mu}}_{ri} \cdot \overline{H}_i. \tag{2}$$

The MSW assumption has been widely used for the analysis and design of YIG-tuned devices [13] as well as for the design of numerous ferrite devices [14]. It is based on the assumption that MSW's can propagate inside a ferrite body, and have a slow phase velocity when compared with the electromagnetic wave. As a consequence, the electric flux density in the second Maxwell's equation (1b) is neglected [15], but the first Maxwell's equation is still present (the MSW fields in YIG devices do not obey the equations of the statics [16], [17]). Hence, in the areas where no source of current is present, the curl of the magnetic field is zero, which is equivalent to say that the magnetic field derives from a scalar potential noted

$$\Psi_i: \quad \overline{H}_i = -\nabla \Psi_i. \tag{3}$$

By virtue of (1c) and (2), this scalar potential has to satisfy

$$\nabla \cdot (\overline{\overline{\mu}}_{ri} \cdot \nabla \Psi_i) = 0. \tag{4}$$

B. Expression of Poynting Theorem

Multiplying the first Maxwell's equation written in layer i by the complex conjugate $\overline{H}_i^*$ of the magnetic field inside this layer and the complex conjugate of the second one by the electric field $\overline{E}_i$, and subtracting the two resulting equations yields (after rearranging)

$$\nabla \cdot (\overline{E}_i \times \overline{H}_i^*)/2 = -2j\omega B_i \cdot \overline{H}_i^*. \tag{5}$$

Integrating the two sides over the whole space and applying the divergence theorem to the result yields

$$\sum_{i=1}^{n} \oint_{S_i} \frac{(\overline{E}_i \times \overline{H}_i^*)}{2} \cdot \overline{n_{si}}\, dS = -2j\omega \sum_{i=1}^{n} \int_{V_i} \frac{\overline{B}_i \cdot \overline{H}_i^*}{4}\, dV \tag{6}$$

where S_i is the surface enclosing the volume V_i of body i, and $\overline{n_{si}}$ is the normal unit pointing outward the surface S_i.

For a multilayered structure, each body is a planar layer, and the contributions to the surface integrals resulting from the two sides of the interface between layers i and j (common to S_i and S_j) compensate. The continuity of the tangential components of the magnetic and electric field is indeed ensured at the conductor-free part of this interface, while the normal component of the power density vanishes on any perfect conductor lying at this interface. Hence, in the case of a planar multilayered structure, the surface to be considered reduces to the surface enclosing the volume V containing all the layers

$$\begin{aligned} \tfrac{1}{2} \oint_S (\overline{E} \times \overline{H}^*) \cdot \overline{n_s}\, dS &= -2j\omega \sum_{i=1}^{n} \int_{V_i} \frac{\overline{B}_i \cdot \overline{H}_i^*}{4}\, dV \\ &= -2j\omega \sum_{i=1}^{n} W_{mi}. \end{aligned} \tag{7}$$

The right-hand side of (6) is, in fact, the summation of the magnetic energy W_{mi} contained inside each volume V_i. When volume V contains an homogeneous medium, (6) reduces to the classical Poynting theorem where the electric flux density has been neglected. Hence, the MSW hypothesis is equivalent to neglecting the electric energy in the Poynting theorem.

Also, under the MSW assumption, the total magnetic energy associated with MSW and present in the right-hand side of (7) may be rewritten using (2) and (3) as

$$\begin{aligned} W_m &= \sum_{i=1}^{n} W_{mi} = \frac{\mu_o}{4} \sum_{i=1}^{n} \int_{V_i} (-\nabla \Psi_i)^* \cdot \{\overline{\overline{\mu}}_{ri} \cdot (-\nabla \Psi_i)\}\, dV_i. \end{aligned} \tag{8}$$

We prove in the Appendix that when using (8), $(4W_m/\mu_o)$ is variational with respect to the scalar potential Ψ_i associated with MSW's in each layer.

C. Comments

From the proof in the appendix, we conclude that the first-order error made on W_m vanishes when the exact magnetic potential Ψ_i associated with MSW's is replaced by a trial one noted Ψ_i^t, provided that:

1) trial potential satisfies (4);
2) trial potential is continuous at the conductor-free part of any interface between two adjacent media having different constitutive parameters;
3) trial induction field obtained as $\overline{\overline{\mu}}_{ri} \cdot (-\nabla \Psi_i^t)$ has continuous normal components at the conductor-free part of such an interface;
4) on a perfect conductor present on a portion of such an interface, either the continuity of the product $(\Psi^t)^* \overline{B}^t \cdot \overline{n_{si}}$ or the cancellation of the normal component of the trial induction field is ensured.

It should be emphasized that no assumption has been made on the dielectric and magnetic properties of the materials. The derivation indeed neither requires complex conjugates of the tensors nor their transposition: the Hermitian nature of $\overline{\overline{\varepsilon}}$ and $\overline{\overline{\mu}}$ is not invoked here. Hence, the expression is variational even when losses are present in the media. Our proof departs from that presented by Collin [12] in three ways. First, the formulation applies to the magnetic energy, and not to the electrostatic energy. Collin indeed mentions the stationary character of both the electrostatic and magnetostatic energies, but gives a proof for the electrostatic energy only. In our case, however, the energy which is calculated is the magnetic energy, and not only the magnetostatic one corresponding to a dc case: the frequency dependence is present in each component of the permeability tensor of the gyrotropic layers. This energy has also been mentioned to be stationary by Davies, but no proof was provided. Davies [18] proposes the use of the variational character of the right-hand side of (8) to deduce some variational expressions for the resonant frequency of cavities. Second, the proof has been extended to inhomogeneous media, which was not done by Collin. Finally, the proof is shown to be valid even when lossy

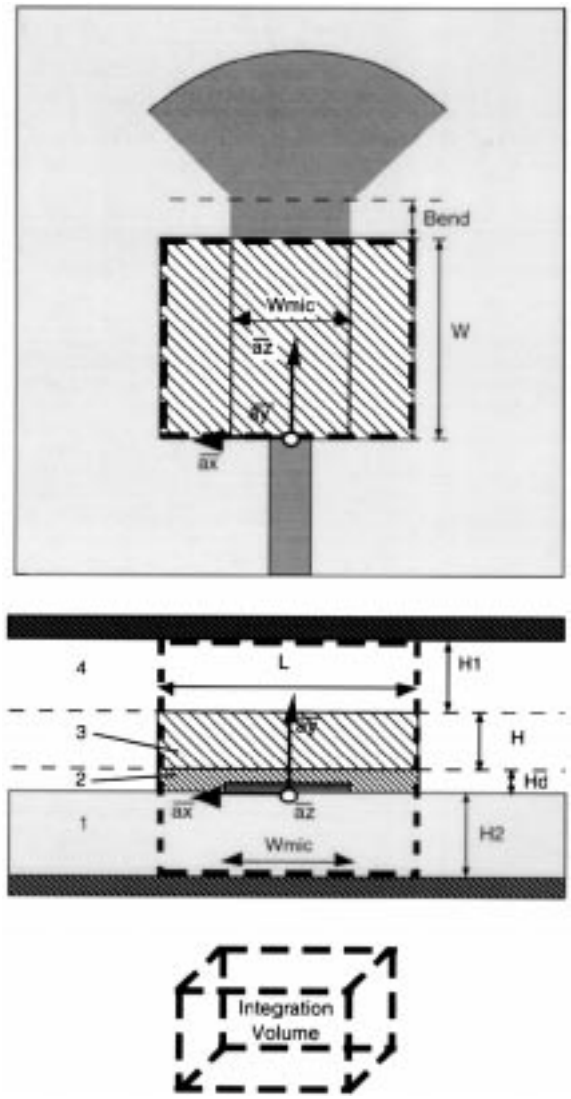

Fig. 1. Topology of one-port YIG SER supporting MSFVW. (a) Top view. (b) Transverse geometry. (c) Perspective view showing the volume considered for the integration: sides are represented by dashed lines in Fig. 1(a) and (b).

gyrotropic media are present, because the conditions rendering W_m stationary do not imply any restriction on the constitutive parameters. Hence, our formulation is well suited for analyzing planar gyrotropic resonators operating at X-band.

III. Application for Designing Planar MSW Gyrotropic Resonators

A. Topology Under Scope

Fig. 1 depicts the top-coupled topology designed by the authors for obtaining an overcoupled behavior of the resonator at the main resonance. It consists of a square piece of a YIG film (3) lying on a square quartz spacer (2) having the same area. The two samples are positioned on a microstrip stub, ended by a wide-band RF short circuit, in order to keep the transverse magnetic field inside the strip close to a maximum in the area covered by the YIG sample. A maximum of coupling is thus expected at X-band. Assuming a propagation of MSW in the z-direction of Fig. 1, three implicit

TABLE I
Gyrotropic Parameters of YIG Film in Fig. 1

Gyrotropic parameters of YIG film		
Saturation magnetization	$4\pi M_s$	1780 Gauss
linewidth	ΔH	1.25 Oe
gyromagnetic ratio	g	2.8 MHz/Oe

TABLE II
Geometrical Dimensions of Breadboard in Fig. 1

Geometrical parameters of breadboard	
thickness of YIG film	H = .100 mm
size of YIG film	L = W = 0.85 mm
thickness of dielectric spacer	H_d = 0.120 mm
thickness of microstrip substrate	H_2 = 0.254 mm
width of microstrip	W_{mic} = 0.420 mm
distance from YIG to upper pole	H_1 = 0. 926 mm

dispersion relations are obtained when the film is considered as infinite in both the x- and z-directions, depending on the orientation of the uniform dc biasing magnetic field H_o [15]. A forward-volume MSW occurs when H_o is y-oriented. Two magnetic poles are thus necessary to bias the YIG film and generate magnetostatic forward-volume waves (MSFVW's). The microstrip substrate is grounded by the bottom pole, assumed to be a perfect electric conductor at RF frequencies. The upper pole acts as a perfect conductive top cover for the RF structure. Hence, the structure has four layers, the first two being low-loss isotropic dielectric substrates, while the third one is a lossy gyrotropic (hence, non-Hermitian) substrate, and the upper layer is air. Layers 1, 2, and 4 have isotropic (diagonal) dielectric and magnetic constitutive tensors

$$\overline{\overline{\varepsilon}}_i = \varepsilon_o \varepsilon_{ri} \overline{\overline{I}}, \qquad \text{for } i = 1, 2, 3, 4$$

and

$$\overline{\overline{\mu}}_i = \mu_o \overline{\overline{I}}, \qquad \text{for } i = 1, 2, 4$$

while the permeability tensor of the third layer has the form

$$\overline{\overline{\mu}}_3 = \mu_o \begin{bmatrix} \mu_{xx,3} & 0 & \mu_{xz,3} \\ 0 & 1 & 0 \\ \mu_{zx,3} & 0 & \mu_{xx,3} \end{bmatrix} \tag{9}$$

with $\mu_{xz,3} = -\mu_{zx,3}$ and $\overline{\overline{\mu}}_3 \neq (\overline{\overline{\mu}}_3)^{T*}$. Expressions for the complex components of $\overline{\overline{\mu}}_3$ are given in [19], as a function of the YIG film parameters and of the biasing dc magnetic field. The YIG film parameters and the geometrical dimensions of the breadboard are reported in Tables I and II.

B. Definition of the Enclosing Surface S

At the edges of the YIG film, the equivalent boundary condition is a perfect magnetic wall. This condition is fixed by the demagnetizing effect occurring on the dc field at the lateral sides of the SER: as a consequence, the tangential components of the magnetic field vanish on the lateral sides of the SER, as stated by [20]. Hence, we find a sufficient condition to be satisfied by both the exact and trial tangential fields on the lateral sides of the sample

$$H_{xi} = -\frac{\partial \Psi_i}{\partial x} = H_{yi} = -\frac{\partial \Psi_i}{\partial y} = 0, \quad \text{at } z = 0 \text{ and } z = W \tag{10a}$$

$$H_{zi} = -\frac{\partial \Psi_i}{\partial z} = H_{yi} = -\frac{\partial \Psi_i}{\partial y} = 0, \quad \text{at } x = -\frac{L}{2} \text{ and } x = \frac{L}{2}. \tag{10b}$$

By choosing the surface enclosing the global volume V as the one containing those lateral sides, one easily satisfies the proper boundary conditions on surface S ensuring that the error (A16) vanishes. This will be shown later.

C. Choice of the Trial Field and Potentials

We start from (4), which has to be satisfied by the trial magnetic potential in each layer. For a z-directed dc magnetic field as in Fig. 1, this equation, denoted Walker's equation in the literature, is rewritten as

$$\mu_{xx,i}\left[\frac{\partial^2 \Psi_i}{\partial x^2} + \frac{\partial^2 \Psi_i}{\partial z^2}\right] + \frac{\partial^2 \Psi_i}{\partial y^2} = 0. \tag{11}$$

A general solution for this equation is [16]

$$\Psi_i = [A \sin k_x x + B \cos k_x x][C_i e^{s_{0i} y} + D_i e^{-s_{0i} y}] \cdot [E \sin k_z z + F \cos k_z z] \tag{12}$$

$s_{0i} = \sqrt{\mu_{xx,i}(k_x^2 - \gamma^2)}$ being the wavenumber along the y-axis k_x, k_z wavenumbers along the x- and z-axis, respectively. It describes the distribution of microwave MSW potentials in multilayered magnetized matter. It has to be noted that MSFVW propagation occurs in the frequency range for which the real part of $\mu_{xx,3}$ is negative.

The interface containing the strip has to be treated separately because of the nonhomogeneous boundary condition on this area. As is done in [21] and [22], we work in the spectral domain, using for this the x-Fourier-transform of (12) for the potential

$$\tilde{\Psi}_i(k_x, y, z) = [C_i(k_x) e^{s_{0i} y} + D_i(k_x) e^{-s_{0i} y}][E \sin k_z z + F \cos k_z z] \tag{13}$$

from which we obtain the spectral form of the three magnetic-field components

$$\tilde{H}_{xi}(k_x, y, z) = -jk_x \tilde{\Psi}_i(k_x, y, z) \tag{14a}$$

$$\tilde{H}_{yi}(k_x, y, z) = -\frac{\partial \tilde{\Psi}_i(k_x, y, z)}{\partial y} = -s_{0i}[C_i(k_x) e^{s_{0i} y} - D_i(k_x) e^{-s_{0i} y}] \cdot [E \sin k_z z + F \cos k_z z] \tag{14b}$$

$$\tilde{H}_{zi}(k_x, y, z) = -\frac{\partial \tilde{\Psi}_i(k_x, y, z)}{\partial z} = -k_z[C_i(k_x) e^{s_{0i} y} + D_i(k_x) e^{-s_{0i} y}] \cdot [E \cos k_z z - F \sin k_z z]. \tag{14c}$$

According to our proof in the appendix, a suited trial-potential rendering (8) variational has to satisfy the continuity of the trial potential and of the normal component of the induction field at conductor-free interfaces between different layers inside the volume V. For the configuration of Fig. 1, the B_y component has to be continuous at various interfaces. We obtain a first set of boundary conditions to be satisfied by the trial potential and induction field, hence, by their spectral form by virtue of the linearity of the Fourier-transform

at $y = H_d$:

$$\tilde{B}_{y2}(k_x, H_d, z) = \tilde{B}_{y3}(k_x, H_d, z) \tag{15}$$

$$\tilde{\Psi}_2(k_x, H_d, z) = \tilde{\Psi}_3(k_x, H_d, z) \tag{16}$$

at $y = H_d + H$:

$$\tilde{B}_{y3}(k_x, H_d + H, z) = \tilde{B}_{y4}(k_x, H_d + H, z) \tag{17}$$

$$\tilde{\Psi}_3(k_x, H_d + H, z) = \tilde{\Psi}_4(k_x, H_d + H, z). \tag{18}$$

We assume that the top and bottom magnetic poles are perfect electric conductors, and impose that the normal induction field has to vanish on them as follows:

at $y = -H_2$:

$$\tilde{B}_{y1}(k_x, -H_2, z) = 0 \tag{19}$$

at $y = H_d + H + H_1$:

$$\tilde{B}_{y4}(k_x, H_d + H + H_1, z) = 0. \tag{20}$$

A nonhomogeneous boundary condition holds at the interface containing the strip. We assume that a trial current density $\overline{J}$ is flowing on the strip, and that its x-dependence is known

$$\overline{J} = J_x(x, z)\overline{ax} + J_z(x, z)\overline{az} \tag{21}$$

with $J_x(x, z) = J_z(x, z) = 0$ for $|x| > W_{\text{mic}}/2$. Hence, its spectral form is also known

$$\tilde{\overline{J}} = \tilde{J}_x(k_x, z)\overline{ax} + J_z(k_x, z)\overline{az}. \tag{22}$$

The magnetic field deduced from the trial potential via (3) has to satisfy a relationship involving the current density

$$\tilde{H}_{x2}(k_x, 0, z) - \tilde{H}_{x1}(k_x, 0, z) = \tilde{J}_z(k_x, z) \tag{23}$$

$$\tilde{H}_{z2}(k_x, 0, z) - \tilde{H}_{z1}(k_x, 0, z) = \tilde{J}_x(k_x, z) \tag{24}$$

while the normal component of the induction field may be imposed continuous

$$\tilde{B}_{y1}(k_x, 0, z) = \tilde{B}_{y2}(k_x, 0, z). \tag{25}$$

Equation (14c) shows that the spectral dependence of the z-component of the magnetic field remains proportional to the spectral trial potential, and a condition sufficient to satisfy the continuity of $(\Psi^t)^* \overline{B}^t \cdot \overline{n_{si}}$ at interface $y = 0$ is to choose $\tilde{J}_x(k_x, z) = 0$. This condition makes the z-component of the magnetic field (hence, of the trial potential) continuous, and the product $(\Psi^t)^* \overline{B}^t \cdot \overline{n_{si}}$ is continuous by virtue of (25). Another solution is to keep $\tilde{J}_x$ unknown, and to subtract the integral (A15) from the energy, after having computed the fields.

Solving the set of equations resulting from the boundary conditions yields an expression for each coefficient $C_i(k_x)$, $D_i(k_x)$ which is proportional to the trial z-component of the current density. Introducing those coefficients into (13) and (14) yields the spectral trial potential and its derived magnetic-field components.

By virtue of (14) for the magnetic field, we see that satisfying boundary conditions (10) on the enclosing surface S is equivalent to impose that the MSW potential vanishes on the lateral sides of the enclosing surface S. Hence, the z-dependence of the potential (trial and true) is

$$\sin k_z z, \qquad \text{with } k_z = n\pi/W. \tag{26}$$

The presence of perfect magnetic walls at $x = \pm(L/2)$ is expressed in the spectral domain by imposing that [22]

$$k_x = (2m+1)\pi/L. \tag{27}$$

Hence, the combination of the boundary conditions (10) on the lateral sides of the surface S and of the boundary conditions (19) and (20) on the bottom and top surfaces of the volume ensures that the error (A16) vanishes.

The obtained spectral potentials and fields in each layer are introduced in the right-hand side of W_m, as explained in [22]. We make use of Parseval identity relating the integral of a product of two functions to the integral of the product of their Fourier transform. The magnetic energy W_m in (7) is rewritten as a function of spectral quantities as

$$\begin{aligned} W_m &= \frac{\mu_o}{4}\sum_{i=1}^{n}\int_{V_i}(-\nabla\Psi_i)^*\cdot\{\overline{\overline{\mu}}_{ri}\cdot(-\nabla\Psi_i)\}\,dV_i \\ &= \frac{\mu_o}{8\pi}\sum_{k_x}\sum_{i=1}^{m}\iint(-\nabla\tilde{\Psi}_i)^* \\ &\quad\cdot\left\{\overline{\overline{\mu}}_{ri}\left(-jk_x\tilde{\Psi}_i, -\frac{\partial\tilde{\Psi}_i}{\partial y}, -\frac{\partial\tilde{\Psi}_i}{\partial z}\right)\right\}\Delta k_x\,dy_i\,dz_i. \end{aligned} \tag{28}$$

In our case, the spectral integration on k_x is replaced by a summation on discrete values for k_x because of the boundary conditions (27) applying to the trial potential on the lateral sides of the sample.

D. Expression for the Reflection Coefficient

We relate this spectral variational form of the magnetic energy to the input impedance of the one-port top-coupled SER configuration in the following manner. Defining at the input access equivalent current I_{in} and voltage V_{in} related by an input impedance Z_{in}, we equate the power flow inside of the surface S to the circuit-oriented definition of this power flow

$$\frac{1}{2}\oint_S(\overline{E}\times\overline{H}^*)\cdot\overline{n_s}\,dS = \frac{1}{2}V_{\text{in}}I_{\text{in}}^* = \frac{1}{2}Z_{\text{in}}|I_{\text{in}}|^2. \tag{29}$$

Combining (7), (8), and (29) yields the final expression of the input impedance

$$\begin{aligned} Z_{\text{in}} &= \frac{-j\omega\mu_o}{8\pi|I_{\text{in}}|^2}\sum_{k_x}\sum_{i=1}^{n}\iint(-\nabla\tilde{\Psi}_i)^* \\ &\quad\cdot\left\{\overline{\overline{\mu}}_{ri}\left(-jk_x\tilde{\Psi}_i, -\frac{\partial\tilde{\Psi}_i}{\partial y}, -\frac{\partial\tilde{\Psi}_i}{\partial z}\right)\right\}\Delta k_x\,dy_i\,dz_i. \end{aligned} \tag{30}$$

Keeping in mind that the trial potentials and fields are proportional to the current density flowing on the strip, by virtue of (23) and (24), we express the input current as the integral of the x-dependence of the trial current density

$$|I_{\text{in}}| = \int_{-W_{\text{mic}}/2}^{W_{\text{mic}}/2} J_z(x)\,dx. \tag{31}$$

From the input impedance Z_{in} the reflection coefficient at the input of the one-port is easily calculated

$$\Gamma_{\text{in}} = \frac{Z_{\text{in}} - Z_o}{Z_{\text{in}} + Z_o} \tag{32}$$

where Z_o is the reference impedance. We take it equal to 50 Ω.

IV. Results

A. Experimental Validation

Fig. 2 shows a comparison between a simulation based on this model [see Fig. 2(a)] and measurements [see Fig. 2(b)] carried out by Alcatel-Bell, Hoboken, Belgium [23], on the configuration presented in Section III-A. The simulation takes into account the geometrical and physical parameters of the various layers and of the shielding, including their losses. As expected, the simulated reflection coefficient [see Fig. 2(a)] of the configuration exhibits an overcoupled behavior: the phase undergoes a sudden drop of 360° at the resonance. Hence, this configuration has been selected for YTO's because the high coupling level yields the oscillation condition over a wide frequency range. The agreement between simulation [see Fig. 2(a)] and experiment (see Fig. 2b) validates the use of the variational formulation (7), (8) in the case of lossy gyrotropic layers. The value of the dc-biasing external magnetic field used for the measurement is $H_o = 5280$ Oe. It induces an internal dc field of 3500 Oe. It has to be noted that this value is used for the computation of the tensor component $\mu_{xx,3}$. A perfect prediction of the resonant frequency is observed.

B. Illustration of the Variational Behavior

Simulated results in Fig. 2 use the well-known current distribution

$$\begin{aligned} J_z(x) &= \frac{1}{\sqrt{1-(2x/W_{\text{mic}})^2}}, \qquad \text{for } |x| < W_{\text{mic}}/2 \\ &= 0, \qquad \text{for } |x| > W_{\text{mic}}/2 \end{aligned} \tag{33a}$$

having the corresponding Fourier transform

$$\tilde{J}_z(k_x) = J_o(k_x W_{\text{mic}}/2). \tag{33b}$$

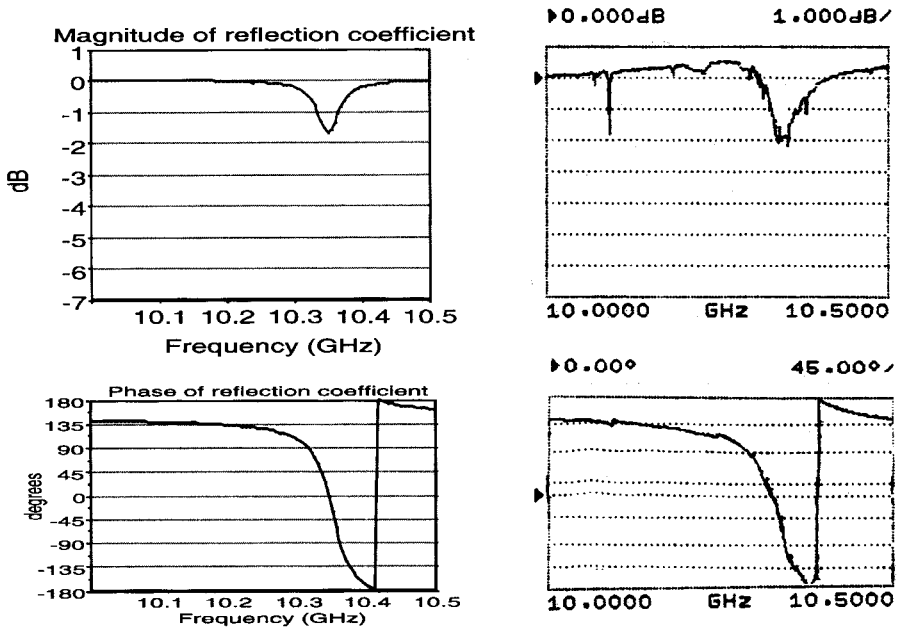

(a) (b)

Fig. 2. Results obtained using variational formulation (26)–(28) applied to the topology of Fig. 1. (a) Magnitude and phase of simulated input reflection coefficient. (b) Magnitude and phase of measured reflection coefficient. DC magnetic field inside YIG film is 3500 Oe for simulation and measurement.

We have also compared results obtained using two different trial potentials, resulting from two different shapes of the trial current density J_z. The first is given by (33), and the second is the uniform current density defined by

$$J_z(x) = 1, \qquad \text{for } |x| < W_{\text{mic}}/2$$
$$= 0, \qquad \text{for } |x| > W_{\text{mic}}/2 \tag{34a}$$

which has as Fourier transform

$$\tilde{J}_z(k_x) = \frac{\sin(k_x W_{\text{mic}}/2)}{k_x W_{\text{mic}}/2}. \tag{34b}$$

Fig. 3 shows the comparison, expressed as the relative difference between the magnitudes of the reflection coefficients computed using (33) and (34), respectively. This difference never exceeds 1.3%, and the error around the resonance is mainly due to a slight shift of resonant frequency induced by the change of current distribution. Hence, the shape of the trial current and potentials has no significant influence on the reflection coefficient computed using (30)–(32). Such a result was expected as a consequence of our proof in the appendix.

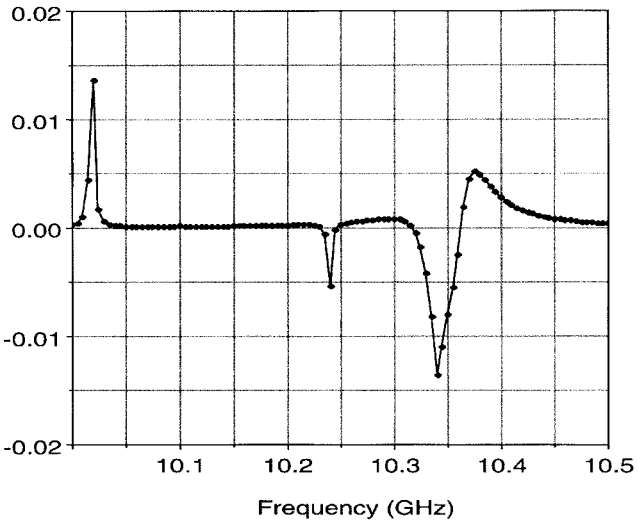

Fig. 3. Relative difference between magnitudes of reflection coefficients simulated using two current densities (33) and (34), respectively.

V. Conclusions

We have developed an efficient energetic variational formulation for the input impedance of MSFVW resonators, containing lossy gyrotropic YIG films. The formulation is based on the proof of the variational character of the magnetic energy associated with MSW's, which remains valid even when non-Hermitian lossy media are present. The excellent agreement observed between theory and measurement validates the use of this model for designing YTO devices. The model was indeed used by the authors in the frame of an ASTP-4 contract funded by the European Space Agency, Estec, The Netherlands. Designs obtained using this model have been presented in [24]. The model is presently modified in order to design wide-band YTO in coplanar-waveguide technology. It has to also be mentioned that the model can be adapted to other types of MSW (surface- or backward-volume waves), obtained by changing the orientation of the applied dc field, because there is no restriction on the permeability tensor. Hence, a number of other configurations will be investigated in the future.

Appendix

We consider (8) and intend to prove that $(4W_m/\mu_o)$ is variational with respect to the scalar potential Ψ_i associated with MSW's in each layer. Varying W_{mi} and Ψ_i in each layer

and rearranging yields

$$K(W_{mi}+\delta W_{mi}) = \int_{V_i}\Big[(-\nabla(\delta\Psi_i+\Psi_i))^*\cdot\{\overline{\overline{\mu}}_{ri}\cdot(-\nabla\delta\Psi_i)\} + (-\nabla\delta\Psi_i)^*\cdot\{\overline{\overline{\mu}}_{ri}.(-\nabla\Psi_i)\}\Big]\,dV_i + \int_{V_i}(-\nabla\Psi_i)^*\cdot\overline{\overline{\mu}}_{ri}\cdot\{(-\nabla\Psi_i)\}\,dV_i \tag{A1}$$

with $K=(4/\mu_o)$.

Keeping in mind that the trial magnetic potential in each layer is defined as

$$\Psi_i^t=\Psi_i+\delta\Psi_i \tag{A2}$$

we may rewrite the error on the magnetic energy as

$$K\delta W_{mi} = \int_{V_i}\Big[(-\nabla\Psi_i^t)^*\cdot\{\overline{\overline{\mu}}_{ri}\cdot(-\nabla\delta\Psi_i)\} + (-\nabla\delta\Psi_i)^*\cdot\overline{\overline{\mu}}_{ri}\cdot(-\nabla\Psi_i)\}\Big]\,dV_i = \delta W1_{mi}+\delta W2_{mi}. \tag{A3}$$

We then use Green's identity

$$\overline{a}\cdot\nabla\Psi+\Psi\nabla\cdot\overline{a}=\nabla\cdot(\overline{a}\Psi) \tag{A4}$$

and transform the two terms of (A3) into

$$K\delta W1_{mi} = \int_{V_i}\nabla\cdot[(\Psi_i^t)^*\{\overline{\overline{\mu}}_{ri}\cdot(\nabla\delta\Psi_i)\}] - (\Psi_i^t)^*\nabla\cdot\{\overline{\overline{\mu}}_{ri}\cdot(\nabla\delta\Psi_i)\}\,dV_i = -\oint_{S_i}(\Psi_i^t)^*\{\overline{\overline{\mu}}_{ri}\cdot(-\nabla\delta\Psi_i)\}\cdot\overline{n_{si}}\,dS_i - \int_{V_i}(\Psi_i^t)^*\nabla\cdot\{\overline{\overline{\mu}}_{ri}\cdot(\nabla\delta\Psi_i)\}]\,dV_i \tag{A5}$$

$$K\delta W2_{mi} = \int_{V_i}[\nabla\cdot[(\delta\Psi_i)^*\{\overline{\overline{\mu}}_{ri}\cdot(\nabla\Psi_i)\}] - (\delta\Psi_i)^*\nabla\{\overline{\overline{\mu}}_{ri}\cdot(\nabla\Psi_i)\}]\,dV_i = -\oint_{S_i}(\delta\Psi_i)^*\{\overline{\overline{\mu}}_{ri}\cdot(-\nabla\Psi_i)\}\overline{n_{si}}\,dS_i - \int_{V_i}(\delta\Psi_i)^*\nabla\{\overline{\overline{\mu}}_{ri}\cdot(\nabla\Psi_i)\}]\,dV_i. \tag{A6}$$

The volume integral in $\delta W2_{mi}$ vanishes because the exact potential Ψ_i satisfies (4). Similarly, the volume integral in $\delta W1_{mi}$ vanishes by imposing

$$\nabla\cdot\{\overline{\overline{\mu}}_{ri}\cdot(-\nabla\delta\Psi_i)\}=0 \tag{A7}$$

which is equivalent to impose that the trial magnetic potential Ψ_i^t defined by (A2) satisfies (4), since the exact potential does. Under this assumption, we obtain the global error made on the energy as a summation of the integrals on the surfaces S_i enclosing each volume V_i:

$$K\delta W_m = K\sum_{i=1}^{n}(\delta W1_{mi}+\delta W2_{mi}) = \sum_{i=1}^{n}\Big[\oint_{S_i}(-\Psi_i^t)^*\{\overline{\overline{\mu}}_{ri}\cdot(-\nabla\delta\Psi_i)\}\cdot\overline{n_{si}}\,dS_i + \oint_{S_i}(-\delta\Psi_i)^*\{\overline{\overline{\mu}}_{ri}.(-\nabla\Psi_i)\}\cdot\overline{n_{si}}\,dS_i\Big]. \tag{A8}$$

Noting $\overline{B}_i$, the exact induction field, and $\overline{B}_i^t$, the trial one, we finally obtain

$$K\delta W_m = \sum_{i=1}^{n}\Big[\oint_{S_i}(-\Psi_i^t)^*(\overline{B}_i^t-\overline{B}_i)\cdot\overline{n_{si}}\,dS_i + \oint_{S_i}(-\delta\Psi_i)^*\overline{B}_i.\overline{n_{si}}\,dS_i\Big]. \tag{A9}$$

We note Ω_{ij}, the interface between layer i and j, which is common to S_i and S_j. The union of the parts of S_i and S_j having no interfaces in common forms the surface S, enclosing the global volume V, and we rewrite (A9) as

$$K\delta W_m = \oint_S(-\Psi^t)^*(\overline{B}^t-\overline{B})\cdot\overline{n_s}\,dS+\oint_S(-\delta\Psi)^*\overline{B}\cdot\overline{n_s}\,dS + \sum_{i=1}^{n-1}\int_{\Omega_{ij}}[(-\Psi_i^t)^*(\overline{B}_i^t-\overline{B}_i)-(-\Psi_j^t)^*(\overline{B}_j^t-\overline{B}_j)]\cdot\overline{n_{si}}\,d\Omega_{ij} + \sum_{i=1}^{n-1}\int_{\Omega_{ij}}\{(-\delta\Psi_i)^*\overline{B}_i-(-\delta\Psi_j)^*\overline{B}_j\}\cdot\overline{n_{si}}\,d\Omega_{ij}. \tag{A10}$$

As for the derivation of the magnetostatic form (6) of the Poynting theorem, we first study the behavior of (A9) and (A10) at interfaces between layers i and j. Two areas have to be considered.

1) No conductors are present between layers i and j. Then, the normal component of the exact induction field and the exact magnetic potential are continuous on the two sides of this conductor-free area of Ω_{ij}

$$\overline{B}_j\cdot\overline{n_{si}}=\overline{B}_i\cdot\overline{n_{si}} \tag{A11}$$

$$\Psi_i=\Psi_j \tag{A12}$$

and the second term of (A10) is rewritten as (neglecting the second-order terms $\delta\Psi_i(\overline{B}_i^t-\overline{B}_i)$ and $\delta\Psi_j^*(\overline{B}_j^t-\overline{B}_j)$)

$$\sum_{i=1}^{n-1}\int_{\Omega_{ij}}(-\Psi_i)^*[(\overline{B}_i^t-\overline{B}_i)-(\overline{B}_j^t-\overline{B}_j)]\cdot\overline{n_{si}}\,d\Omega_{ij} = \sum_{i=1}^{n-1}\int_{\Omega_{ij}}(-\Psi_i)^*(\overline{B}_i^t-\overline{B}_j^t)\cdot\overline{n_{si}}\,d\Omega_{ij} \tag{A13}$$

by virtue of (A11).

This term vanishes, provided that the trial induction field has normal components continuous at the conductor-free part of Ω_{ij}.

The third term of (A10) is rewritten as

$$\sum_{i=1}^{n-1}\int_{\Omega_{ij}}\{(\delta\Psi_j-\delta\Psi_i)^*\overline{B}_i\}\cdot\overline{n_{si}}\,d\Omega_{ij}. \tag{A14}$$

By virtue of (A12), this term will vanish, provided that the trial magnetic potential is continuous at the conductor-free part of Ω_{ij}.

2) On the perfect conductors, the normal component of the exact induction field vanishes as follows:

$$\overline{B}_i \cdot \overline{n_{si}} = \overline{B}_j \cdot \overline{n_{sj}} = 0, \qquad \text{with} \quad \overline{n_{si}} = -\overline{n_{sj}}.$$

On that area of Ω_{ij}, the second term of (A10) simplifies into

$$\sum_{i=1}^{n-1} \int_{\Omega_{ij}} \{(-\Psi_i^t)^* \overline{B}_i^t - (-\Psi_j^t)^* \overline{B}_j^t\} \cdot \overline{n_{si}}\, d\Omega_{ij} \qquad \text{(A15)}$$

while the third one vanishes.

Hence, a sufficient condition to make the second term of (A10) vanish on the perfect conductor is either to make the product $(\Psi^t)^* \overline{B}^t \cdot \overline{n_{si}}$ continuous at the interface Ω_{ij}, or subtract its integral (A15) from (8), as is classically done in [25], or to make the normal component of the trial induction field vanish at the perfect conductor. Finally, under such assumptions, the error made on the global energy reduces to the integral on the surface S enclosing the global volume V and may be rewritten, to the second-order error, as

$$K\delta W_m = \oint_S (\Psi^t)^* (\overline{B}^t - \overline{B}) \cdot \overline{n_s}\, dS + \oint_S (\delta\Psi)^* \overline{B} \cdot \overline{n_s}\, dS. \qquad \text{(A16)}$$

Hence, an efficient way to cancel δW_m is to impose that the volume considered is such that Ψ^t and Ψ vanish on its enclosing surface S, or that both the trial and true induction fields vanish.

ACKNOWLEDGMENT

The authors are grateful to Dr. M. Guglielmi and Dr. F. Coromina, European Space Agency, Estec, The Netherlands, Prof. A. Vander Vorst, Microwaves Université Catholique de Louvain (UCL), Louvain-la-Neuve, Belgium, and Dr. P. Van Loock, Alcatel-Bell, Hoboken, Belgium, for fruitful discussions.

REFERENCES

[1] A. K. Ganguly and D. C. Webb, "Microstrip excitation of magnetostatic surface waves: Theory and experiment," *IEEE Trans. Microwave Theory Tech.*, vol. MTT-23, pp. 998–1006, Dec. 1975.
[2] P. R. Emtage, "Interaction of magnetostatic waves with a current," *J. Appl. Phys.*, vol. 49, no. 8, pp. 4475–4484, Aug. 1978.
[3] J. D. Adam and S. N. Bajpai, "Magnetostatic forward volume wave propagation in YIG strips," *IEEE Trans. Magn.*, vol. MAG-18, pp. 1598–1600, Nov. 1982.
[4] I. J. Weinberg, "Insertion loss for magnetostatic volume waves," *IEEE Trans. Magn.*, vol. MAG-18, pp. 1607–1609, Nov. 1982.
[5] K. W. Chang and W. S. Ishak, "Magnetostatic forward volume wave straight edge resonator," in *IEEE MTT-S Int. Microwave Symp. Dig.*, 1986, pp. 473–475.
[6] I. W. O'Keefe and R. W. Paterson, "Magnetostatic surface waves propagation in finite samples," *J. Appl. Phys.*, vol. 49, pp. 4886–4895, 1978.
[7] W. Ishak and K. W. Chang, "Tunable microwave resonators using magnetostatic wave in YIG films," *IEEE Trans. Microwave Theory Tech.*, vol. MTT-34, pp. 1383–1393, Dec. 1986.
[8] I. Huynen, G. Verstraeten, and A. Vander Vorst, "Theoretical and experimental evidence of nonreciprocal effects on magnetostatic forward volume wave resonators," *IEEE Microwave Guided Wave Lett.*, vol. 5, pp. 195–197, June 1995.
[9] K. Kurokawa, *An Introduction to the Theory of Microwaves Circuits.* New York: Academic, 1969, ch. 4.
[10] R. F. Harrington, *Time-harmonic Electromagnetic Fields.* New York: McGraw-Hill, 1961, pp. 431–435.
[11] J. Schwinger and D. S. Saxon, *Discontinuities in Waveguides—Notes on Lectures by J. Schwinger*. New York: Gordon and Breach, 1968.
[12] R. E. Collin, *Field Theory of Guided Waves*, 2nd ed. Piscataway, NJ: IEEE Press, 1991, ch. 2, pp. 12–14.
[13] P. Kabos and V. S. Stalmachov, *Magnetostatic Waves and Their Applications.* London, U.K.: Chapman & Hall, 1994.
[14] J. Helszajn, *Principles of Microwaves Ferrites Engineering.* New York: Wiley, 1969.
[15] P. Kabos and V. S. Stalmachov, *Magnetostatic Waves and Their Applications.* London, U.K.: Chapman & Hall, 1994, ch. 1, pp. 33–37.
[16] R. W. Damon and J. R. Eshbach, "Magnetostatic modes of a ferromagnetic slab," *Int. J. Phys. Chem. Solids*, vol. 19, no. 12, pp. 1308–1320, 1961.
[17] P. Kabos and V. S. Stalmachov, *Magnetostatic Waves and Their Applications.* London, U.K.: Chapman & Hall, 1994, ch. 1, pp. 34–35.
[18] J. B. Davies in T. Itoh, *Numerical Methods for Microwave and Millimeter Wave Passive Structures.* New York: Wiley, 1989, ch. 2.
[19] B. Lax and K. J. Button, *Microwaves Ferrites and Ferrimagnetics.* New York: McGraw-Hill, 1962.
[20] J. P. Parekh, K. W. Chang, and H. S. Tuan, "Propagation characteristics of magnetostatic waves," in *Circuits, Syst. Signal Processing*, vol. 4, 1985, no. 1/2, pp. 9–38.
[21] P. Kabos and V. S. Stalmachov, *Magnetostaticwaves and Their Applications.* London, U.K.: Chapman & Hall, 1994, ch. 2, p. 67.
[22] I. Huynen, D. Vanhoenacker, and A. Vander Vorst, "Spectral domain form of new variational expression for very fast calculation of multilayered lossy planar line parameters," *IEEE Trans. Microwave Theory Tech.*, vol. 42, pp. 2099–2106, Nov. 1994.
[23] G. Verstraeten, private communication, June 1993.
[24] G. Verstraeten, J. Marien, and F. Coromina, "Low phase-noise tunable oscillators using magnetostatic wave resonators," in *Proc. 26th European Microwave Conf.*, Prague, Czech Republic, Sept. 1996, pp. 90–93.
[25] A. D. Berk, "Variational principles for electromagnetic resonators and waveguides," *IEEE Trans. Antennas Propagat.*, vol. AP-4, pp. 104–111, Apr. 1956.

Isabelle Huynen was born in Brussels, Belgium, in 1965. She received the degree in electrical engineering and the Ph.D. degree in applied sciences from the Université Catholique de Louvain (UCL), Louvain-la-Neuve, Belgium, in 1989 and 1994, respectively.

In 1989, she joined the Microwave Laboratory, UCL. Her research deals with electromagnetic theory using variational principles and measurement techniques applied to microwave and millimeter-wave structures and materials.

Benoît Stockbroeckx was born in Schaerbeek, Belgium, in 1970. He received the engineer degree in electrical engineering (for his thesis, he investigated the S-matrix characterization of microwave-optical transducers) and the Ph.D. degree in applied sciences from the Université Catholique de Louvain (UCL), Louvain-la-Neuve, Belgium, in 1993 and 1998, respectively.

In 1993, he joined the Microwave Laboratory, UCL, where his research interest was microwave planar-circuits modeling. From 1993 to 1994, he investigated YIG resonators modeling. Since 1994, his research interests are related to the wide-band slotline antennas and Vivaldi antenna modeling.

Guy Verstraeten was born in Antwerp, Belgium, in 1961. He received the degree in physical engineering from the Université of Ghent, Ghent, Belgium, in 1986.

Since 1988, he has been with Alcatel Bell, Space Systems Department, Hoboken, Belgium, where his research deals with technological and design aspects of various microwave components and systems for satellite communications.